Polarized Infrared Attenuated Total Reflection for the in Situ Determination of the Orientation of Surfactant Adsorbed at the Solid/Solution Interface

David J. Neivandt,[†] Michelle L. Gee,*[,†] Michael L. Hair,[‡] and Carl P. Tripp*[,‡]

School of Chemistry, University of Melbourne, Parkville, Victoria, 3052, Australia, and Xerox Research Centre of Canada, 2660 Speakman Drive, Mississauga, Ontario, Canada, L5K2L1

Received: January 16, 1998

Polarized infrared attenuated reflection (IR-ATR) has been used to determine the average orientation of the methylene tail of cetyltrimethylammonium bromide (CTAB) adsorbed at the silica/solution interface under both equilibrium and nonequilibrium conditions, in situ. The equilibrium orientation was measured over the pH range of 2−10. It was found that the equilibrium orientation of the surfactant was larger at higher pH values owing to an increase in the packing density with increasing surface excess. The evolution of the orientation of the surfactant at the interface during the adsorption process was monitored at a pH of 9.2. To the authors' knowledge, this is the first time that nonequilibrium changes in the molecular orientation of surfactants adsorbing at the solid/solution interface have been determined in situ. During the initial stage of adsorption, there was no preferred orientation of the surfactant, but as the surface excess increased with time, the surfactant began to orient in a direction more normal to the surface. This change in orientation was rapid. Desorption of this CTAB layer by addition of poly(styrenesulfonate) was slow and led to a 90% desorption. The residual 10% of surfactant retained the orientation of the original highly packed layer and relaxed slowly to a more random configuration only after an extended period of time. This suggests that the extraction of the surfactant by poly(styrenesulfonate) occurs in localized areas and that the surfactant remaining on the surface is found in highly packed patches or clusters.

Introduction

Surfactant adsorption at the solid/solution interface is used to modify the surface properties and hence interfacial behavior in industrial areas such as colloidal dispersion/flocculation in mineral processing, soil treatment, the pharmaceutical industry, the cosmetics industry, food processing, and detergency.[1] In general, surfactant adsorption is employed to modify a surface in order to promote a desired interaction with another surface or species. A knowledge of quantities such as the surface coverage, the degree of surface charge neutralization, the internal structure of the adsorbed layer, and the kinetics of adsorption as a function of solution conditions is therefore required.

Many techniques may be used to measure properties of an adsorbed film on a surface. Adsorbed amounts, and hence adsorption isotherms, may be determined by titration measurement of the residual adsorbate in solution[2] or by direct spectroscopic studies of the adsorbed species.[3,4] While surface coverage is important, many of the properties of a surface in solution are regulated by the residual surface charge. Accurate determination of surface charge and potential is possible using methods such as electrophoresis[5] and the direct measurement of surface forces.[6]

Some knowledge of the quality and orientation of a thin film formed at the solid/solution interface may be obtained by contact angle measurements, although these must of necessity be performed ex situ. Microproperties of adsorbed layers on solid substrates may be determined for example by fluorescence,[7] electron spin resonance,[8] and nuclear magnetic resonance.[9] The extension of an adsorbed layer in the direction normal to the surface at the solid/solution interface may be measured in situ by ellipsometry,[10] neutron reflectivity,[11] or direct force measurements.[12]

Orientational information of adsorbed molecules has been determined by several techniques, although most are experimentally demanding and often require removal of the film from solution. Near edge X-ray absorption fine structure[13] (NEXAFS) and angle-dependent X-ray photon spectroscopy[14] (XPS) are capable of providing film thickness and average orientation of alkyl chains at a surface, although the measurements are performed under vacuum. Neutron reflectivity has the potential to provide composition profiles of adsorbed molecules normal to the surface in situ.[15] This requires isotopic labeling of sections of the adsorbed molecule. The power of the technique is aided by the ability to control the level of deuteration of the solvent to provide a zero contribution from the solvent.[16] The major drawback of neutron reflectivity is the limited access to a neutron source. Sum frequency vibrational spectroscopy[17,18] and waveguide Raman scattering[19] are powerful techniques that have been successfully applied to orientational studies of adsorbed surfactants, although again both require equipment not readily available in most laboratories.

One of the most powerful and easily applied techniques for the determination of surface excesses and orientational information of species adsorbed at the solid/solution interface is infrared attenuated total reflection (IR-ATR). The total internal reflection of an infrared beam at the solid/solution interface produces an evanescent wave of the same frequency in the interfacial region of the solution. An adsorbed molecule that absorbs in the infrared region will attenuate the reflected beam, and an absorbance spectrum of the adsorbed species is obtained. For

* Authors to whom correspondence should be addressed.
[†] University of Melbourne.
[‡] Xerox Research Centre of Canada.

S1089-5647(98)00801-3 CCC: $15.00
Published on Web 06/05/1998

many years the technique has been applied to the study of surface active species, although usually ex situ. Calibration of the internal reflection element has allowed the determination of surface excesses of adsorbed molecules,[20] and some information on the nature of the film formed has been obtained by studying shifts in band positions and shape.[21,22]

Extending standard IR-ATR to incorporate polarization allows determination of the molecular orientation of adsorbed species. Polarization of the internally reflected beam results in the production of an evanescent wave that has electric field amplitudes in either the plane of the surface (S polarization) or in the direction normal to the surface (P polarization). Comparison of the absorbance of an oscillator in the two polarizations allows the determination of the orientation of the transition moment with relation to the surface. If the internal geometry of the absorbing species is known, then the orientation of the species may be calculated. Polarized IR-ATR has been successfully applied to the determination of molecular orientations in many systems. Langmuir−Blodgett[23,24] and self-assembled films[25] of a wide range of surface active molecules have been investigated ex situ at the solid/air interface on a variety of metal oxide surfaces. Polarized IR-ATR has also been applied to the study of lipid monolayers and bilayers at both the air/water[26] and lipid/water[27] interface.

However, few in situ attempts have been made to monitor the orientation of surfactants adsorbed at the solid/solution interface, particularly from aqueous solution. This may be attributed to several experimental difficulties that are encountered when attempting such measurements. The primary concern is the small signal obtained from monolayer or submonolayer coverages on low surface area substrates. This may be countered to some extent by the use of multiple internal reflection elements and high-sensitivity spectrometers. Contributions from residual adsorbate in bulk solution to the absorbance spectra of the adsorbed species may be significant and must be considered. Further complications may arise from the optical transmission properties of the substrate and solution, both of which are usually low in the frequency range at which the absorption is monitored. This problem is often encountered when silicon is used as the internal reflection substrate. Silicon is a desirable material to use since its surface may be oxidized to produce a silica surface.[28] The optical cutoff of silicon is at approximately 1550 cm^{-1}, making difficult the detection of many functional groups. Sperline et al.[29] have circumvented this problem by sputtering a thin layer of silicon on a germanium internal reflection element. The technique produces a substrate with essentially the transmission properties of germanium but with the surface chemistry of silicon. An alternative to studying functional groups in the low-frequency region is to monitor the methylene stretching bands of a polymer backbone or surfactant tail. Most infrared substrates are highly transmitting in this frequency region (2800−3000 cm^{-1}), although solvent absorption may be problematic. This is a particular problem in aqueous solution, as the methylene stretching modes lie on the edge of a broad water absorption band.

When following the kinetics of an adsorption process, there are additional experimental limitations to those mentioned above since many spectra must be collected over the time scale of the adsorption process. Furthermore, to monitor the evolution of the orientation of an adsorbing species, one must determine the absorption in two planes from the interface in rapid succession. The use of polarization modulation techniques employing a photoelastic modulator[30] or a polarizing beamsplitter[31] may avoid this problem but have yet to be applied to kinetics studies. Nevertheless, the time constraints produce a trade-off in the signal-to-noise ratio of spectra that is dependent on the speed of sampling. For these reasons the few IR-ATR studies of the kinetics of adsorption of surfactants have not employed polarization techniques.[32,33] Several studies on polymer orientational kinetics have been performed by polarized IR-ATR; these are generally somewhat simplified by the typically longer adsorption times and higher signal strengths involved.[34,35]

In this paper we present in situ polarized IR-ATR measurements of the 2920 cm^{-1} (asymmetric) and 2850 cm^{-1} (symmetric) methylene bands of the surfactant cetyltrimethylammonium bromide (CTAB) adsorbed on the silica surface of a silicon internal reflection element from aqueous solution. Absorbance values in the two planes of polarization are measured and information regarding the orientation of adsorbed CTAB determined. The average orientation of the surfactant is followed kinetically during adsorption and equilibrium orientations determined over a range of pH values.

Experimental Section

Apparatus. IR-ATR spectra were taken using a twin parallel mirror reflection attachment for multiple internal reflections supplied by Harrick Scientific Corp. A 50 × 20 × 2 mm 45° trapezoidal silicon internal reflection element (IRE) was used. The IRE was housed in a stainless steel flow-through cell sealed by two Kalrez o-rings. The solution was contained in an external reservoir equipped with a pH probe and stirrer and was introduced to the silicon IRE via a peristaltic pump and Teflon flow tubing. This setup allowed for ease in changing solution conditions without disruption of the cell position.

A thin oxide layer was prepared on the surface of the silicon IRE, according to a procedure outlined elsewhere.[36] In brief, preparation of the IRE for an experiment involved the following steps: refluxing in concentrated nitric acid for 5 h to remove any organic residue, rinsing with water, boiling in a 10% by volume concentrated NH_3 in 30% (w/v) H_2O_2 solution for 15 min to create a fresh oxide layer, and further copious rinsing with "Milli-Q" water. The stainless steel cell was passivated using concentrated nitric acid and rinsed thoroughly with "Milli-Q" water before use. All fittings and tubing were soaked in concentrated NaOH for 24 h. Glassware was detergent washed and treated with concentrated HNO_3 before final rinsing.

Spectra were collected using a Bomem Michelson 110 FT-IR spectrometer, as modified by Tripp and Hair.[37] Polarization was achieved by two wire grid polarizers (ZnSe and KRS-5) mounted on a three-position slide mechanism. The polarizers (on two of the three positions of the slide) were set to perpendicular (S) and parallel (P) polarization of the IR beam with reference to the plane of incidence of the IRE, while the third position of the slide was open to allow collection of nonpolarized spectra. The desired polarization of the beam could then be achieved simply by sliding the shuttle holding the polarizers into the correct position. See Figure 1 for a schematic representation of the internal reflection cell and beam polarization setup. Even though throughput for the nonpolarized IR-ATR setup relative to the open beam was only 6.5%, a peak-to-peak noise level of 2×10^{-4} absorbance units in the 3000−2800 cm^{-1} region was obtained for a single 1 s scan. Typically 1000 scans were coadded, giving a peak-to-peak noise level of 6×10^{-6} absorbance units for equilibrium measurements. Kinetic measurements were made by collection of ten 1 s scans, which were coadded at each of the three slide positions, i.e., S, P, and nonpolarized.

The protocol adopted for the experiments was as follows: The IRE was installed in the cell, the flow lines connected, and

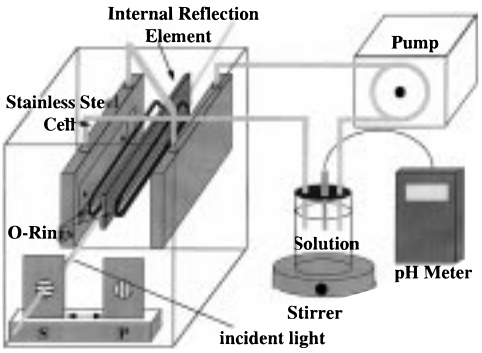

Figure 1. Schematic representation of the IR-ATR experimental apparatus. The main feature to note is that the incident light is passed through a polarizer to polarize in either the S plane or the P plane.

the assembly mounted in the spectrometer and aligned. The cell was then filled with "Milli-Q" water and allowed to stabilize for 24 h to ensure full hydroxylation of the surface. S, P, and nonpolarized reference spectra were then taken, and a freshly prepared sample solution was introduced. If orientational kinetics were to be monitored, collection of S, P, and nonpolarized spectra commenced immediately upon solution entering the cell. Final spectra of an experimental solution under given solution conditions were taken 24 h after introduction to the cell in order to allow adequate time for adsorption equilibrium to occur.

Materials. Cetyltrimethylammonium bromide was supplied by Eastman Kodak and was further purified by double recrystallization from an acetone/ethanol mixture. Poly(styrenesulfonate) with a molecular weight of 199 000 and a polydispersity of 1.08 was used as supplied by Pressure Chemical Company, Pittsburgh. Solution preparation and final rinsing of components was with water from a "Milli-Q" water purification system. Adjustment of solution pH was achieved through analytical reagent grade hydrochloric acid and sodium hydroxide.

Theory. Attenuated total reflection (ATR) arises from the internal reflection of an electromagnetic wave at the interface between two optically transparent media of different refractive index. If the wave strikes the interface from within the higher refractive index medium at an angle, θ, greater than the critical angle (as defined by Snell's law), then total internal reflection occurs. An electromagnetic disturbance with exponentially decreasing intensity is produced normal to the surface in the lower refractive index medium upon total internal reflection. This wave is known as an evanescent wave. If the evanescent wave interacts with an absorbing species, then the beam reflected from the interface within the higher refractive index medium is attenuated. It is this attenuation that is measured in ATR experiments.

Figure 2 is a schematic representation of total internal reflection, with the conventional axis system defined. The refractive indices of medium one and medium two are n_1 and n_2, respectively such that $n_1 > n_2$. The internally reflected beam is defined as being in the $x-z$ plane, which is known as the plane of incidence. The $x-y$ plane is that of the surface and is orthogonal to the plane of incidence, as depicted in Figure 2. Polarization of the incident beam may result in an evanescent wave polarized in either the plane of incidence, which is defined as parallel or P polarization, or in the plane of the surface, that is perpendicular or S polarization. Parallel (P) polarization results in electric field amplitude components of the evanescent wave in the x and z axis, E_x, and E_z. Conversely, perpendicular (S) polarization produces an evanescent wave with an electric field amplitude solely in the y axis, E_y. Values of the electric

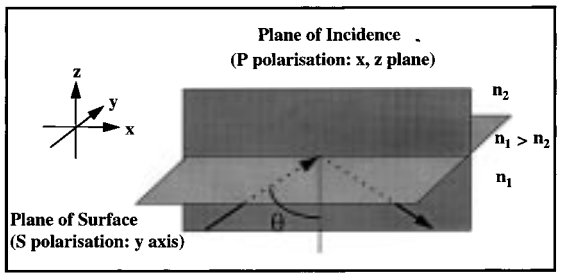

Figure 2. Schematic representation of polarized IR-ATR. The ATR element, with refractive index n_1, lies in the $x-y$ plane. Total internal reflection of the incident light through the ATR element, as indicated by the arrows, results in production of an evanescent wave in the medium of refractive index n_2. The evanescent wave can be P polarized (polarized in the $x-z$ plane) or S polarized (polarized in the $x-y$ plane).

field amplitude components in each of the three axes are dependent only upon the refractive index properties of the system and the angle of incidence of the totally internally reflected beam.

The degree to which an absorbing species interacts with the evanescent wave is dependent on the alignment between the plane in which its transition moments lies and the plane of polarization of the evanescent wave. It is therefore possible to determine the orientation of an absorbing species with relation to the surface, simply by measuring its absorbance in the two planes of polarization. The ratio of absorbance in the S and P polarization states is often given the notation A_s/A_p and is referred to as the dichroic ratio.

It is possible to predict A_s/A_p ratios of transition moments in given orientations to the surface by relating the plane of orientation to the electric field amplitude components of the appropriate planes of polarization. These calculated A_s/A_p ratios may be compared to experimental data to determine the orientation of absorbing molecules in real systems. In this manner a molecule aligned with transition moments in the plane of the surface (as would be the case for the CH_2 groups of a methylene surfactant tail orientated normal to the surface) has a predicted A_s/A_p ratio of

$$\frac{A_s}{A_p} = \frac{E_y^2}{E_x^2} \tag{1}$$

A molecule with no preferential transition moment alignment has a predicted A_s/A_p ratio of

$$\frac{A_s}{A_p} = \frac{E_y^2}{E_x^2 + E_z^2} \tag{2}$$

Calculation of the electric field amplitudes in the x, y, and z axis therefore allows determination of the A_s/A_p ratios expected for each of the molecular orientations considered above by simple substitution. The electric field amplitudes of the evanescent wave at the interface in each of the three axes may be calculated given that the angle of incidence of the reflected beam (θ) and the refractive index properties of the system are known. The angle of incidence of the beam at the interface is fixed by the angle of the beveled face of the internal reflection element. Determination of the refractive index properties of the interfacial region is complicated by the presence of an oxide layer of silica on the silicon substrate and by the possibility of the adsorption of surfactant significantly altering the refractive index at the surface from that of bulk solution. In order to account for these possibilities, the system is modeled in terms

of a varying number of successive layers of different refractive index and the electric field amplitudes and hence A_s/A_p ratios are determined for each. The calculated A_s/A_p ratios may then be compared to experimental results of molecules in known orientations and the model best matching the real system determined.

Two-Layer Refractive Index Model. The simplest way of modeling the system is to consider it to be composed of two layers: an optically dense medium (the internal reflection element) of refractive index n_1 and a less dense medium (bulk solution) with a refractive index n_2. The electric field amplitudes at the interface for such a system are given by[38]

$$E_x = \frac{2(\cos\theta)[\sin^2\theta - {n_{21}}^2]^{1/2}}{(1-{n_{21}}^2)^{1/2}[(1+{n_{21}}^2)\sin^2\theta - {n_{21}}^2]^{1/2}} \quad (3)$$

$$E_y = \frac{2\cos\theta}{(1-{n_{21}}^2)^{1/2}} \quad (4)$$

$$E_z = \frac{2\sin\theta\cos\theta}{(1-{n_{21}}^2)^{1/2}[(1+{n_{21}}^2)\sin^2\theta - {n_{21}}^2]^{1/2}} \quad (5)$$

where $n_{21} = n_2/n_1$. Substitution of refractive index values for our apparatus, $n_1 = 3.42$ (silicon), $n_2 = 1.33$ (water), and $\theta = 45°$, results in values of E_x, E_y, and E_z that upon substitution into eqs 1 and 2 give predicted A_s/A_p ratios of 1.22 for oscillators in the plane of the surface and 0.50 for oscillators of no preferred orientation.

Three-Layer Refractive Index Model. Incorporation of a thin layer of organic material of refractive index 1.50 intermediate between the silicon surface and solution requires the use of a three-layer model for calculation of electric field amplitudes and, hence, A_s/A_p ratios. The electric field amplitude components for the three-layer model are given by[23]

$$E_x = \frac{2(\cos\theta)[\sin^2\theta - {n_{31}}^2]^{1/2}}{(1-{n_{31}}^2)^{1/2}[(1+{n_{31}}^2)\sin^2\theta - {n_{31}}^2]^{1/2}} \quad (6)$$

$$E_y = \frac{2\cos\theta}{(1-{n_{31}}^2)^{1/2}} \quad (7)$$

$$E_z = \frac{2(\sin\theta\cos\theta){n_{32}}^2}{(1-{n_{31}}^2)^{1/2}[(1+{n_{31}}^2)\sin^2\theta - {n_{31}}^2]^{1/2}} \quad (8)$$

where $n_{31} = n_3/n_1$ and $n_{32} = n_3/n_2$. Substitution of $n_1 = 3.42$ (silicon), $n_2 = 1.50$ (organic layer), and $n_3 = 1.33$ (water) into eqs 6, 7, and 8, followed by insertion of the resulting electric field amplitude values into eqs 1 and 2, gives predicted A_s/A_p ratios of 1.22 and 0.65 for perpendicular and random orientations of transition moments to the surface, respectively.

A final consideration is the presence of a thin oxide layer on the silicon internal reflection element. If a three-layer model is employed for the silicon/silica/solution system and the refractive index, n_2, of silica is 1.41, then an A_s/A_p ratio of 0.57 is predicted for random orientation of the absorbing species, with the perpendicular A_s/A_p value remaining unchanged at 1.22.

Results

We have shown previously[36] that despite the large sampling depth of the evanescent wave in comparison to the adsorbed layer thickness, the contribution to absorbance signals from species in bulk solution at the surfactant concentrations employed (5.5×10^{-5} M) is less than 5%. This leads to only small errors in the surface excesses determined via ATR absorbance measurements, for our particular system, and hence the contribution from bulk solution has been ignored in the presentation of the results, below.

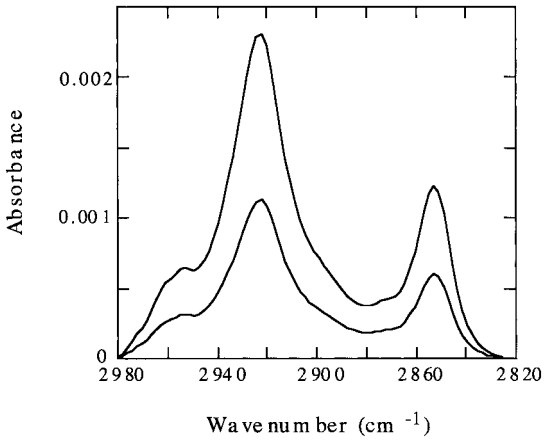

Figure 3. Polarized IR-ATR absorbance spectra of 5.0×10^{-4} M isotropic CTAB solution at pH 1.7. The lower spectrum is obtained when the beam is S polarized. The upper spectrum is obtained when the beam is P polarized.

S and P polarized IR-ATR spectra of an isotropic CTAB solution provide a means of confirming the validity of the predicted A_s/A_p ratio for random surfactant orientation. A series of CTAB solutions of concentrations from 5.5×10^{-5} to 9×10^{-4} M were introduced successively from low to high concentration to the flow-through cell and S and P polarized spectra collected. Figure 3 is a typical set of spectra measured in the S and P polarization states (lower and upper curves, respectively) for 5×10^{-4} M CTAB solution at pH 1.7. The experiment was performed at a pH of 1.7 since it is known that CTAB does not adsorb on silica at this pH value,[36] and thus any measured absorbance is due only to surfactant in bulk solution. Additionally, surfactant in bulk solution is isotropic; the A_s/A_p ratio should be 0.5, as predicted above for random orientation using the two-layer silicon/solution model. At all concentrations, the A_s/A_p ratio of the 2920 cm^{-1} CTAB band was 0.50 ± 0.03, confirming our theoretical predictions of this ratio.

It is noted that the A_s/A_p ratio for random orientation determined by the three-layer model for the silicon/silica/solution system of 0.57 is considerably greater than the above measured value of 0.50 ± 0.03. It is concluded from this result that the deviation from the two-layer model caused by the presence of the silica layer is small and may be deemed insignificant. As shall be seen in a following section on the kinetics of adsorption, CTAB adsorbed on the oxide surface of the internal reflection element at low surface excesses gave A_s/A_p ratios lower than the value of 0.65 expected for random orientation using the three-layer silicon/organic/solution model. This suggests that the presence of a thin layer of organic material on the oxide surface does not appreciably perturb the evanescent wave. At higher surface excesses, the A_s/A_p ratio rapidly rises above the 0.65 value, which may imply either that the surfactant assumes a degree of order in the direction normal to the surface or that the increased adsorbed amount does perturb the evanescent wave and that the system may no longer be approximated by a simple two-layer model of refractive indices. To clarify this point, a thin layer of the polyelectrolyte, poly(styrenesulfonate), was cast onto the oxide surface and its A_s/A_p ratio measured in aqueous solution. A value of 0.50 was measured at methylene surface

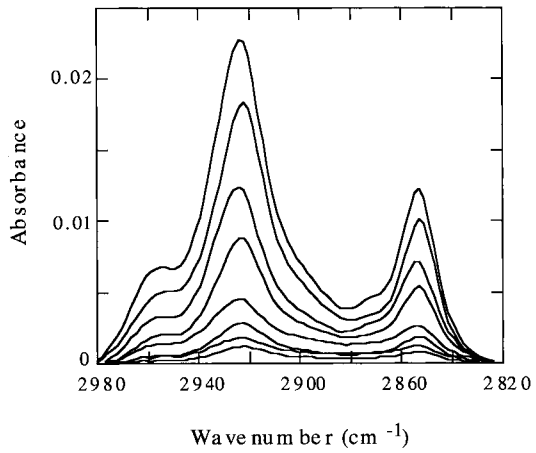

Figure 4. Polarized IR-ATR absorbance spectra of equilibrated CTAB adsorbed from 5.5×10^{-5} M solution at pH's 2.1, 4.9, 7.4, and 9.6. The lower spectrum at each pH is obtained when the beam is S polarized. The upper spectrum is obtained when the beam is P polarized.

TABLE 1: Surface Excess and Ratio of Absorbance in the S and P Polarized States (A_s/A_p Ratio) of the 2920 cm^{-1} Methylene Band of CTAB Adsorbed from 5.5×10^{-5} M Solution at pH's 2.1, 4.9, 7.4, and 9.6

pH	Γ (molecules/nm^2)	A_s/A_p ratio
2.1	0.05	0.67
4.9	0.32	0.69
7.4	1.71	0.75
9.6	3.04	0.79

excess values far higher than those measured in the present experiments. This result implies that the presence of a layer of organic material at the interface does not have an appreciable effect on the refractive index properties of our system and that we are justified in using a two-layer silicon/solution model to calculate theoretical values of the A_s/A_p ratio for comparison to our experimental data.

CTAB Orientation at Adsorption Equilibrium. Equilibrium orientations of adsorbed CTAB at pH values in the range 2.1−9.6 were determined in the following manner: a 5.5×10^{-5} M CTAB solution at pH 2.1 was introduced to the cell and the pH raised successively though 4.9 and 7.4 to a final value of 9.6. Nonpolarized and S and P polarized spectra were taken after 24 h to allow sufficient time for adsorption equilibrium to be attained at each pH value. Figure 4 is a plot of the spectra measured in the S and P polarization states at pH's 2.1, 4.9, 7.4, and 9.6. The surface excesses (determined by calibration to previous results[36]) and A_s/A_p ratios of the 2920 cm^{-1} band for each pH are given in Table 1.

It can be seen from the A_s/A_p ratio of 0.67 at pH 2.1 that even at a low surface coverage (0.05 molecules/nm^2) the surfactant is partially ordered in a direction normal to the surface. Raising the pH and hence the surface excess at equilibrium results in an overall increase in alignment toward the normal. This is reflected as a rise in the A_s/A_p ratio.

Kinetics of CTAB Adsorption. The kinetics and orientation of CTAB adsorption on the oxide surface of the IRE at pH 9.6 were followed by monitoring of the nonpolarized and S and P polarized absorbance of the 2920 cm^{-1} band of methylene with time. The nonpolarized absorbance of the 2920 cm^{-1} band and the A_s/A_p ratio are plotted against time on the left and right ordinate axes, respectively, of Figure 5a. It should be noted that the choice of scale and range of the A_s/A_p ratio axis is arbitrary, and thus the close correlation between the absorbance and A_s/A_p ratio curves should not be taken as absolute, although certainly similar trends are observed.

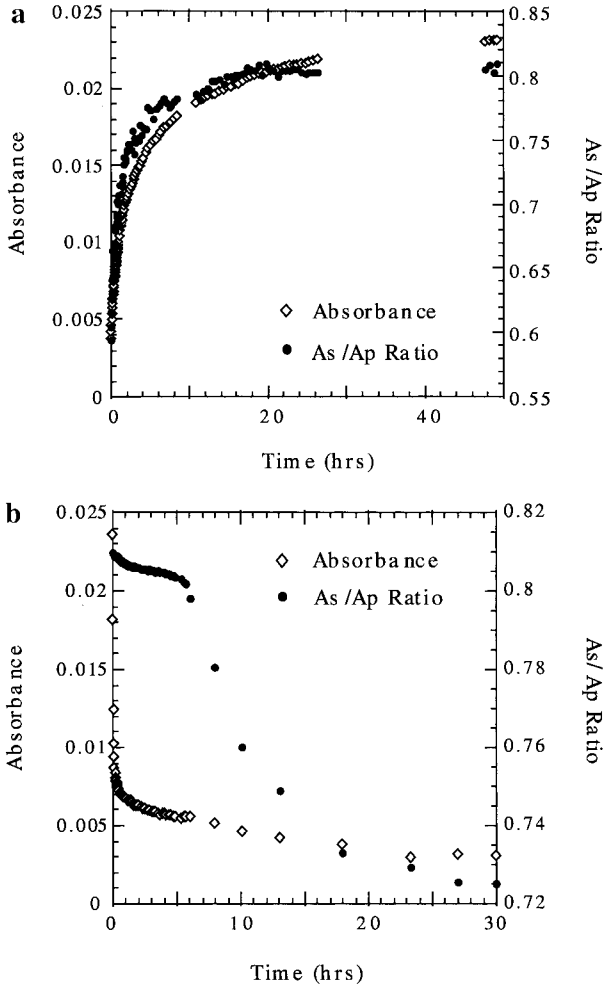

Figure 5. (a) Kinetics of the adsorption of CTAB from a 5.5×10^{-5} M CTAB solution at pH 9.6. The absorbance for a nonpolarized light (left ordinate) and the A_s/A_p ratio (right ordinate) are plotted as a function of time. Absorbance was obtained by monitoring the 2920 cm^{-1} methylene band of CTAB as it adsorbs until equilibrium was attained. (b) Kinetics of the desorption of CTAB from a silica surface due to the addition of 100 ppm poly(styrenesulfonate). The absorbance for a nonpolarized light (left ordinate) and the A_s/A_p ratio (right ordinate) are plotted as a function of time. Absorbance was obtained by monitoring the 2920 cm^{-1} methylene band of CTAB on the surface, until equilibrium was attained.

It may be seen from the nonpolarized absorbance plot that while approximately 80% of the equilibrium amount is adsorbed within 10 h of addition of CTAB solution to the cell, a total in excess of 30 h is required to reach full adsorption equilibrium. From the low A_s/A_p ratios measured at low surface coverages it is evident that the surfactant is randomly orientated during initial adsorption. As the surface excess of CTAB increases with time, the average orientation of the surfactant toward the normal rises, as shown by the increase in the A_s/A_p ratio. A plateau in the A_s/A_p ratio with time is observed at a value of 0.80, corresponding to a plateau in the adsorbed amount.

In order to gain insight into the reordering of residual adsorbed surfactant upon desorption, the polyelectrolyte poly(styrenesulfonate), PSS, was added to the cell at 100 ppm concentration. The strong interaction between the anionic polyelectrolyte and the cationic surfactant results in a very large and rapid desorption of CTAB from the surface. The nonpolarized absorbance of the 2920 cm^{-1} band of methylene is plotted against time on the left ordinate of Figure 5b, while the A_s/A_p ratio is plotted on the right ordinate. Time zero corre-

sponds to the addition of the polyelectrolyte. It is seen that surfactant removal was extremely rapid in the initial stages, gradually decaying to a plateau at approximately 10% of the adsorbed amount prior to PSS addition.

Polarized measurements of the desorption process after PSS addition showed that the A_s/A_p ratio of approximately 0.80 was largely maintained in the residual adsorbed surfactant during the initial rapid desorption. After more than 80% of the surfactant adsorbed at equilibrium had been removed, the A_s/A_p ratio of the residual surfactant began to decrease slowly, eventually reaching a plateau value of 0.73.

Discussion

Figure 3 shows the absorbance spectrum of isotropic CTAB in solution, i.e., CTAB that is not adsorbed at an interface, in both S and P polarized states over the frequency range of the C−H stretching modes. The absorbance bands at 2920 and 2850 cm^{-1} are, respectively, the asymmetric and symmetric C−H stretching vibrations of methylene (CH_2), while the 2960 cm^{-1} band is the asymmetric C−H stretch of the methyl group (CH_3). It can be seen that the S polarized spectrum (lower) is far less intense that the P polarized spectrum (upper), yielding an A_s/A_p ratio of 0.50 ± 0.03 for the 2920 cm^{-1} methylene band of CTAB in isotropic solution. As stated above, this is in agreement with the predicted A_s/A_p ratio, as calculated in the Theory section, and so confirms that the experimental setup is working and that the simple two-layer model of refractive indices predicts the A_s/A_p ratio correctly for isotropic solutions.

The A_s/A_p ratio of 0.67 for CTAB adsorbed at the silica/solution interface at a pH of 2.1 (see Table 1) indicates that CTAB is not isotropic once adsorbed but adopts an orientated structure. This value of 0.67 indictates an average alignment of the adsorbed surfactant normal to the surface. An A_s/A_p ratio of 0.31 is predicted for CTAB lying flat in the plane of the surface and an A_s/A_p ratio of 1.22 for alignment in the plane normal to the surface. The A_s/A_p ratio of 0.67 therefore represents a preferential alignment of CTAB molecules intermediate between these extremes. A theory developed by Axelson et al.[39] allows the calculation of an angle of inclination of the surfactant molecule's methylene tail to the surface from the A_s/A_p ratio. For our system, the measured value of 0.67 corresponds to an angle of 48°. While we cannot confidently apply the theory of Axelson et al. to our system due to the fact that dispersion of the IR beam produces a variety of angles of incidence and therefore a range of penetration depths of the evanescent wave, it nonetheless gives a qualitative indication of what the A_s/A_p ratios imply in terms of surfactant alignment. The value of 48° for the angle of the CTAB tail to the surface suggests a relatively high degree of order. This result is particularly interesting in light of the fact that the surface excess of CTAB is 0.05 molecules/nm^2 (refer to Table 1). Table 1 indicates that a surface excess of approximately 3 molecule/nm^2 corresponds to a close-packed monolayer of CTAB where the molecules are aligned approximately perpendicular to the plane of the surface. At a very low surface excess, it would be expected that the surface would consist of CTAB molecules sparsely distributed across the surface with no packing constraints which might otherwise force them to order, thus leading to a low A_s/A_p ratio. However, even at the low surface excess of 0.05 molecules/nm^2 the molecules are exhibiting some preferred orientation. One possible explanation for this observation is that the adsorption process consists of the formation of small clusters or patches of surfactant molecules on the surface. Hence, within these surfactant-rich patches, the molecules adopt some degree of order.

Table 1 indicates that as the solution pH increases, the amount of CTAB adsorbed increases and there is a corresponding increase in the A_s/A_p ratio. The effect of pH on the adsorbed amount of CTAB is understood in terms of favorable electrostatic interactions between the cationic surfactant and the silica surface, which is known to become increasingly more negatively charged with increasing pH, above its isoelectric point at approximately 2.0−3.0.[40] The increase in the A_s/A_p ratio from 0.67 to 0.79 with the pH change from 2.1 to 9.6 indicates that the surfactant's average orientation becomes progressively more normal to the surface as more surfactant adsorbs. This implies that as a greater number of surfactant molecules are to be accommodated on the surface, the alkyl chains of the surfactant tend to orientate more normally to the surface and so project less area onto the substrate.

Nonpolarized absorbance values of CTAB during the adsorption regime at pH 9.6 are plotted against time on the left ordinate of Figure 5a. These provide an indication of the kinetics of CTAB adsorption on silica. Initial adsorption of the surfactant was very rapid, with approximately 50% of the final equilibrium adsorbed amount being adsorbed within 2 h of introduction of the CTAB solution to the internal reflection cell. The rate of adsorption of the surfactant then began to decrease to the extent that it took a further 8 h to reach 80% of the final adsorbed amount. Adsorption equilibrium was not obtained until approximately 30 h after introduction of the solution to the surface.

The overall orientation of CTAB on the oxide surface was observed to change markedly during the adsorption process. It may be seen from the right ordinate of Figure 5a that during the initial stages of adsorption the surfactant had an A_s/A_p ratio of approximately 0.60, indicative of a low degree of orientation in the direction normal to the surface. As the surface excess increased, the A_s/A_p ratio rose very rapidly, reaching a value of 0.75 within approximately 2 h. Further increases in orientation occurred much more slowly. An A_s/A_p ratio of 0.80 was reached at the plateau, although approximately 30 h was required to reach this value.

The measured change in average orientation of the surfactant over time implies that the CTAB rearranges on the surface to accommodate further adsorption. An alternative explanation for the data is that initial adsorption is close to nonorientated; later adsorption is highly orientated, resulting in a high average A_s/A_p ratio. The former option would result in maximization of the packing density of surfactant at the interface, whereas the latter option would result in a significantly lower packing density, and so full monolayer coverage could not be achieved. The maximum absorbance measured, as shown in Figures 5a, is 0.023. This corresponds to a surface excess of approximately 3 molecules/nm^2. The area per head group of a CTAB molecule is known, from the size of the molecule, to be approximately 0.25 nm^2, and so we would expect to measure a surface excess of 4 molecules/nm^2 assuming the molecules are aligned completely normal to the surface. If we take into account that the maximum measured A_s/A_p ratio of 0.8 indicates that the molecules are aligned at an angle significantly less than 90° to the surface (if alignment were 90°, the A_s/A_p ratio would be 1.22, as calculated above in the theory section), the area per molecule should be somewhat greater than 0.25 nm^2 due to the extra area taken up by the projection of the tilted surfactant tail. For example, if the surfactant molecule is at an angle of 70° to the surface, the length of the tail can be calculated to be approximately 0.5 nm, assuming the CTAB tail is fully extended and is 1.5 nm long.[12] Thus a tilted CTAB molecule would occupy an area of about 0.3 nm^2, leading to an expected

surface excess of 3.3 molecules/nm^2. Any hydration of the head group will further increase the area per molecule expected for a close-packed monolayer. Indeed, monolayer coverage of CTAB on mica has been shown[41] to correspond to an area per molecule of 0.4 nm^2. Hence, the measured surface excess of 3 molecules/nm^2 implies maximization of the packing density. Thus, by monitoring the kinetics of adsorption, we have been able to monitor the rearrangement on the surface of surfactant molecules leading to monolayer formation.

Figure 5b shows the effect of the addition of the anionic polyelectrolyte poly(styrenesulfonate), PSS, to the adsorbed surfactant. The very large and rapid desorption of CTAB from the silica surface upon addition of PSS, as seen by the decrease in the 2920 cm^{-1} band absorbance plotted on the left ordinate of Figure 5b, indicates that the interaction between the polyelectrolyte and the adsorbed surfactant is sufficiently strong to result in the removal of most of the CTAB from the surface. The interaction between CTAB and PSS has been shown to be very strong and cooperative,[42,43] as a result of association of the surfactant tails with the alkyl backbone of the polyelectrolyte and the electrostatic attraction between the cationic surfactant head group and the sulfonate groups of PSS. The implication of this result is that CTAB associates with PSS in preference to adsorption onto silica, even under conditions where the electrostatic interaction between the surfactant head group and the surface is maximized. It is interesting that CTAB is not completely removed from the surface by the addition of PSS; at equilibrium approximately 10% of the original adsorbed amount remains.

Polarized measurements of the desorption process show that the high degree of surfactant orientation that was present prior to PSS addition (A_s/A_p ratio of 0.80) was largely maintained over a 6 h period, during which the adsorbed surfactant decreased to approximately 20% of the equilibrium adsorbed amount. A significant decrease in the A_s/A_p ratio was only observed during the following 25 h, when the equilibrium value for the A_s/A_p ratio plateaued at 0.73, indicating some order in the residual surfactant even though the surface coverage is low. The very slow reorganization of residual adsorbed surfactant is in contrast to the rapid reorientation observed during adsorption. These results suggest that CTAB remaining on the silica surface during the desorption process retains the equilibrium orientation it possessed originally, and it maintains this for a considerable time before relaxing into a less orientated structure at low surface coverages. It should be noted that the very large loss of surfactant from the surface without an immediate correspondingly large decrease in the A_s/A_p ratio also supports our supposition that the surfactant layer does not significantly modify the refractive index properties of the system from those of a two-layer model.

The maintenance of a high A_s/A_p ratio of the residual surfactant upon the initial rapid loss of 80% of the surface excess suggests that the desorption of the surfactant by PSS occurs in localized areas and that any CTAB that does remain on the surface maintains a high degree of order. The residual adsorbed surfactant would be located in isolated patches or clusters on an otherwise bare or sparsely populated surface. Surfactant molecules within these clusters would be expected to maintain a high degree of order since, within an individual cluster, the packing density of surfactant is high, and hence a high A_s/A_p ratio should be maintained.

Summary

We have demonstrated for the first time that polarized infrared attenuated total reflection (IR-ATR) can be used to determine orientational kinetics of surfactants adsorbing and desorbing at the solid/solution interface from aqueous solution in situ. Measurements were made of the methylene absorbance bands of cetyltrimethylammonium bromide (CTAB) adsorbing on silica in the S and P polarized states. The ratio of absorbance in the two polarization states (A_s/A_p) was compared to values calculated for random orientation ($A_s/A_p = 0.50$) and orientation perpendicular to the plane of the surface ($A_s/A_p = 1.22$).

CTAB adsorbed on silica from pure surfactant solution was observed to possess some degree of orientation. Measurement of the A_s/A_p ratios of CTAB adsorbed onto silica as a function of pH indicated that as the surface excess of surfactant increases, there is a trend toward increased alignment of the surfactant normal to the surface. This is attributed to the surfactant packing in a more vertical manner in order to facilitate further CTAB adsorption.

The average orientation of the surfactant was monitored as a function of time during the adsorption process to give an indication of orientational kinetics. On initial adsorption at low surface excesses, the surfactant adsorbs in a near random orientation. As the adsorption process progresses and the adsorbed amount increases, a corresponding and extremely rapid rise in the orientation of the surfactant is observed so as to maximize packing density.

Addition of the polyelectrolyte poly(styrenesulfonate), PSS, produced a very rapid desorption of CTAB where the remaining molecules maintain a high degree of order. The residual surfactant relaxes its orientation only slowly with time, about 30 h being required. This indicates that surfactant desorption occurs in localized areas and that the residual surfactant is present in isolated clusters of highly ordered molecules that take a considerable time to relax their orientation.

Acknowledgment. The authors acknowledge the Australian Research Council for financial support of this project.

References and Notes

(1) Rosen, M. J. *Surfactants and Interfacial Phenomena*; Wiley and Sons: New York, 1978.
(2) Barr, T.; Oliver, J.; Stubbings, W. V. *J. Chem. Soc. Ind.* **1948**, *67*, 45.
(3) Lijour, Y.; Calves, J.-Y.; Saumagne, P. *J. Chem. Soc., Faraday Trans. 1* **1987**, *83*, 3283.
(4) Wangnerud, P.; Olofsson, G. *J. Colloid Interface Sci.* **1992**, *153*, 392.
(5) Hunter, R. J. *Zeta Potential in Colloid Science*; Ottewill, R. H., Rowell, R. L., Eds.; Academic Press: London, 1981.
(6) Israelachvili, J. N.; Adams, G. E. *J. Chem. Soc., Faraday Trans. 1* **1978**, *74*, 975.
(7) Legrange, J. D.; Riegler, H. E.; Zurawsky, W. P.; Scarlata, S. *F. Thin Solid Films* **1988**, *159*, 101.
(8) Esumi, K.; Otsuka, H.; Meguro, K. *J. Colloid Interface Sci.* **1990**, *186*, 224.
(9) Quist, P.-Q.; Soderlino, E. *J. Colloid Interface Sci.* **1995**, *172*, 510.
(10) Zorin, Z. M.; Churaev, N. V.; Esipova, N. E.; Sergeeva, I. P.; Sobolev, V. D.; Gasanov, E. K. *J. Colloid Interface Sci.* **1992**, *152*, 170.
(11) Rennie, A. R.; Lee, E. M.; Simister, E. A.; Thomas, R. K. *Langmuir* **1990**, *6*, 1031.
(12) Rutland, M. W.; Parker, J. L. *Langmuir* **1994**, *10*, 1110.
(13) Bierbaum, K.; Kinzler, M.; Woll, C.; Grunze, M.; Hahner, G.; Heid, S.; Effenberger, F. *Langmuir* **1995**, *11*, 512.
(14) Takahara, A.; Morotomi, N.; Hiraoka, S.; Higashi, N.; Kunitake, T.; Kajiyama, T. *Macromolecules* **1989**, *22*, 617.
(15) Krueger, S.; Ankner, J. F.; Satija, S. K.; Majkrzak, C. F.; Gurley, D.; Colombini, M. *Langmuir* **1995**, *11*, 3218.
(16) Fragneto, G.; Thomas, R. K.; Rennie, A. R.; Penfold, J. *Langmuir* **1996**, *12*, 6036.
(17) Ward, R. N.; Davies, P. B.; Bain, C. D. *J. Phys. Chem.* **1993**, *97*, 7141.
(18) Duffy, D. C.; Davies, P. B.; Creeth, A. M. *Langmuir* **1995**, *11*, 2931.

(19) Rabe, J. P.; Novotny, V.; Swalen, J. D.; Rabolt, J. F. *Thin Solid Films* **1988**, *159*, 359.
(20) Frantz, P.; Leonhardt, D. C.; Granick, S. *Macromolecules* **1991**, *24*, 1868.
(21) Keith, S.; Rochester, C. H. *J. Chem. Soc., Faraday Trans. 1* **1988**, *84*, 3641.
(22) Kung, K.-H. S.; Hayes, K. F. *Langmuir* **1993**, *9*, 263.
(23) Haller, G. L.; Rice, R. W. *J. Phys. Chem.* **1970**, *74*, 4386.
(24) Takenaka, T.; Nogami, K.; Gotoh, H.; Gotoh, R. *J. Colloid Interface Sci.* **1971**, *35*, 395.
(25) Maoz, R.; Sagiv, J. *J. Colloid Interface Sci.* **1984**, *100*, 465.
(26) Pastrana, B.; Mautone, A. J.; Mendelsohn, R. *Biochemistry* **1991**, *30*, 10058.
(27) Vandenbussche, G.; Clercx, A.; Clercx, M.; Curstedt, T.; Johansson, J.; Jornvall, H.; Ruysschaert, J.-M. *Biochemistry* **1992**, *31*, 9169.
(28) Frantz, P.; Granick, S. *Langmuir* **1992**, *8*, 1176.
(29) Sperline, R. P.; Jeon, J. S.; Raghavan, S. *Appl. Spectrosc.* **1995**, *49*, 1178.
(30) Golden, W. G.; Saperstein, D. D.; Severson, M. W.; Overend, J. *J. Phys. Chem.* **1984**, *88*, 572.
(31) Ishida, H.; Ishino, Y.; Buijs, H.; Tripp, C. P.; Dignam, M. J. *Appl. Spectrosc.* **1987**, *41*, 1288.
(32) Yang, R. T.; Low, M. J. D.; Haller, G. L.; Fenn, J. J. *Colloid Interface Sci.* **1973**, *44*, 249.
(33) McKeigue, K.; Gulari, E. *Surfactants in Solution*; Mittal, K. L., Lindman, B., Eds.; Plenum Press: New York, 1984; Vol. 2.
(34) Alston, J. V. *Macromolecules* **1992**, *25*, 3007.
(35) Enriquez, E. P.; Granick, S. *Colloids Surf. A* **1996**, *113*, 11.
(36) Neivandt, D. J.; Gee, M. L.; Hair, M. L.; Tripp, C. P. *Langmuir* **1997**, *13*, 2519.
(37) Tripp, C. P.; Hair, M. L. *Appl. Spectrosc.* **1992**, *46*, 100.
(38) Harrick, N. J. *Internal Reflection Spectroscopy*; Interscience: New York, 1967.
(39) Axelsen, P. H.; Braddock, W. D.; Brockman, H. L.; Jones, C. M.; Dluhy, R. A.; Kaufman, B. K.; Puga, F. J. I. *Appl. Spectrosc.* **1995**, *49*, 526.
(40) Iler, R. K. *The Chemistry of Silica*; Wiley-Interscience: New York, 1979.
(41) Pashley, R. M.; Israelachvili, J. N. *Colloids Surf.* **1981**, *2*, 169.
(42) Almgren, M.; Hansson, P.; Mukhtar, E.; van Stam, J. *Langmuir* **1992**, *8*, 2405.
(43) Fundin, J.; Brown, W. *Macromolecules* **1994**, *27*, 5024.